Biochemistry **2001,** *40,* 7559−7568

Comparative Binding Properties of Metallobleomycins with DNA 10-mers†

Wenbao Li,‡ Chunqing Zhao,‡ Chuanwu Xia,‡ William E. Antholine,§ and David H. Petering*,‡

Department of Chemistry, University of Wisconsin−Milwaukee, P.O. Box 413, Milwaukee, Wisconsin 53201, and National Biomedical ESR Center, Medical College of Wisconsin, 8701 Watertown Plank Road, Milwaukee, Wisconsin 53223

Received August 14, 2000; Revised Manuscript Received January 9, 2001

ABSTRACT: Properties of the interaction of bleomycin (Blm) and metallobleomycins [M = Zn, Cu(II), Fe(III), and HO_2−Co(III)] with site-specific and nonspecific DNA oligomers, d(GGAA**GC**TTCC)$_2$ (**I**) and d(GGAA**AT**TTCC)$_2$ (**II**), respectively, were investigated. With both 10-mers association constants increased in the series Blm A_2, ZnBlm A_2, Cu(II)Blm A_2, Fe(III)Blm A_2, and HO_2−Co(III)Blm A_2. Generally, the metallobleomycins were bound with a modestly higher affinity to **I**. One-dimensional ^{1}H NMR spectra of the imino proton region of **I** in the presence of this series of compounds revealed that Blm and Zn- and CuBlm bind in fast exchange on the NMR time scale, while the Fe and Co complexes bind in slow exchange. Blm, ZnBlm, and Cu(II)Blm caused little perturbation of the UV circular dichroism spectrum of **I** or **II**. In contrast, Fe(III)Blm and HO_2−Co(III)Blm induced hypochromic effects in the CD spectrum of **I** and altered the spectrum of **II** to a smaller extent. On the basis of these results, the DNA binding structures and properties of Blm A_2, ZnBlm A_2, and CuBlm A_2 differ substantially from those of Fe(III)Blm A_2 and HO_2−Co(III)Blm A_2.

Bleomycin is a natural product antitumor agent that undergoes activation by forming an iron complex in cells (Figure 1) (*1*, *2*). FeBlm[1] attacks DNA through the reactive species, HO_2−Fe(III)Blm, causing single and double strand damage as well as base release (*3*−*9*). There is site selectivity to these reactions such that DNA cleavage occurs preferentially at 5′-G-pyrimidine-3′ sites (*10*, *11*). A plausible pathway of reaction in cell nuclei, where the ratio of DNA bases to drug is 10^5 or greater, involves several steps (*12*):

$$\mathrm{Fe(III)Blm + DNA \rightleftarrows Fe(III)Blm{-}DNA} \quad (1)$$

$$\mathrm{Fe(III)Blm{-}DNA + e^- \rightleftarrows Fe(II)Blm{-}DNA} \quad (2)$$

$$\mathrm{Fe(II)Blm{-}DNA + O_2 \rightleftarrows O_2{-}Fe(II)Blm{-}DNA} \quad (3)$$

$$\mathrm{O_2{-}Fe(II)Blm{-}DNA + e^- + H^+ \rightleftarrows HO_2{-}Fe(III)Blm{-}DNA} \quad (4)$$

$$\mathrm{HO_2{-}Fe(III)Blm{-}DNA \rightarrow DNA\ damage + Fe(III)Blm{-}DNA} \quad (5)$$

Reactions 2 and 4 are redox processes with unspecified reducing agents. An understanding of the mechanism of these reactions culminating in DNA damage requires a knowledge of the structures and properties of FeBlm−DNA species that participate in these steps, as well as detailed information about reaction 5. However, relatively little structural information has been obtained about FeBlm species and their DNA adducts (*13*).

Studies of the reaction of dioxygen with Co(II)Blm in the absence and presence of calf thymus DNA or synthesized DNA 10-mers have documented numerous similarities to the reaction of O_2 with Fe(II)Blm (*14*−*17*). Notably, because of the stability and diamagnetic character of HO_2−Co(III)-Blm with DNA, NMR structural analysis of this molecule and its DNA adducts has provided an attractive opportunity to examine a model for HO_2−Fe(III)Blm−DNA (*15*). The three-dimensional structure of HO_2−Co(III)Blm showed it to be a compact, folded molecule in which the metal domain, comprised of A, P, and H components in Figure 1, exists as one of two chiral forms and binds Co(III) with five nitrogen ligands; the sixth, axial position is occupied by hydroperoxide (*18*, *19*). The metal domain and the peptide linker (V, T) form a globular unit (Figure 1) (*20*). Extending from T, the bithiazole moiety (B) partially encloses the hydroperoxide in a pocket that also includes the Co(III) coordination plane and the folded linker region. Completing the structure, the disaccharide (G, M) protrudes above the cobalt coordination plane next to the axial amine group.

NMR structures of HO_2−Co(III)Blm A_2 and HO_2−Co-(III)pepleomycin bound to DNA 10-mers containing 5′-GC-3′ and 5′-GT-3′ sites have been completed (*21*−*23*). In summary, they show that the bithiazole unit intercalates between the base pairs involving C or T and the next base pairs on their 3′ sides and that the pyrimidinyl ligand in the metal coordination plane of the drug makes two hydrogen bonds with G in the minor groove of the DNA duplexes. These latter interactions demonstrate that site specificity is, at least, partly determined through metal domain−DNA

† Supported by NIH Grant CA-22184 (D.H.P.) and NSF Instrumentation Grant BIR-9512622.

* To whom correspondence should be addressed. Telephone: (414) 229-5853. Fax: (414) 229-5530. E-mail:petering@uwm.edu.

‡ University of Wisconsin−Milwaukee.

§ Medical College of Wisconsin.

[1] Abbreviations: Blm, the bleomycin mixture containing both Blm A_2 and B_2 (Figure 1); Blm A_2, the major component of the clinical mixture blenoxane; **I**, d(GGAA**GC**TTCC)$_2$; **II**, d(GGAA**AT**TTCC)$_2$; HEPES, *N*-(2-hydroxyethyl)piperazine-*N*′-2-ethanesulfonic acid; MBlm, metallobleomycin; (M)Blm, Blm or metallobleomycin; Pep, pepleomycin.

10.1021/bi001915t CCC: $20.00
Published on Web 06/02/2001

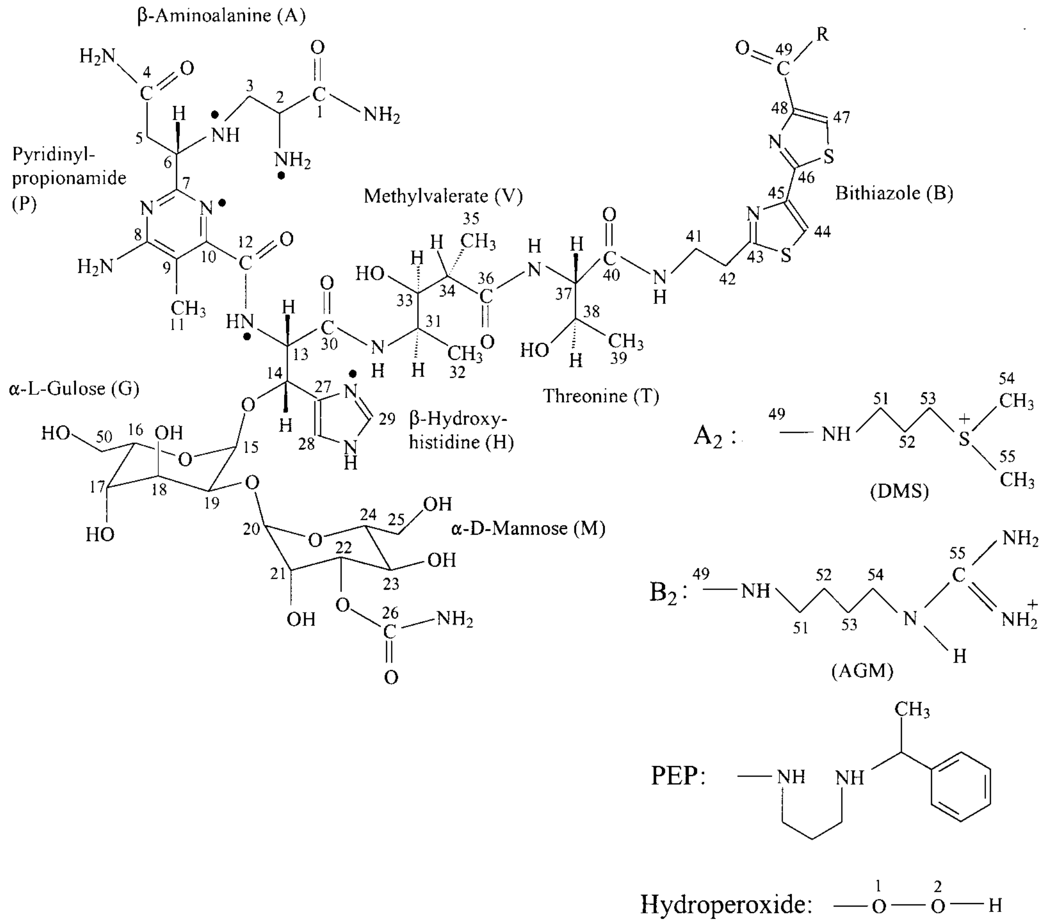

FIGURE 1: Structure of bleomycin. Dots indicate sites of binding of metal ions.

interactions. As a result of binding in this mode, the hydroperoxide is placed in position to attack the H4′ of C or T, which is the known target of reaction of HO_2−Fe(III)-Blm (*21*, *22*).

Investigation of the binding and reaction of several Co- and FeBlms with the self-complementary DNA 10-mers, d(GGAA**GC**TTCC)$_2$ (**I**, specific site) and d)GGAA**AT**TTCC)$_2$ (**II**, nonspecific site) has demonstrated that various properties of their metal domains clearly change as **II** is substituted for **I** (*17*, *24*). These results support the view that both Co- and FeBlms discriminate between sites of nucleotide binding through their metal domains and encourage the hypothesis that CoBlm is a good model for FeBlm.

The objective of the present work is to advance the understanding of the contributions that the metal domain makes to the properties of DNA−drug adducts. The present experiments continue to explore the characteristics of iron and cobalt bleomycins bound to DNA as well as determine comparable properties of Zn- and CuBlm A_2 and Blm A_2. In particular, measurements have been made of the equilibrium constants for the binding of various (M)Blm species to **I** and **II**, the chemical exchange properties of these metallobleomycins when bound to **I**, and the CD spectra of **I** and **II** in the absence and presence of this series of (M)-Blms.

MATERIALS AND METHODS

Blenoxane, the clinical mixture largely made up of Blm A_2 and B_2, was a gift from Bristol Myers Co. Blm A_2 used in this study was isolated from blenoxane according to a published method (*18*). ZnBlm A_2 or CuBlm A_2 were made as one-to-one ratios of Blm and metal ions. Fe(III)Blm A_2 was prepared as previously described and its iron content measured by atomic absorption spectrophotometry (*12*). HO_2−Co(III)Blm A_2 and Co(III)Blm A_2 were produced by reacting Blm A_2 with $CoCl_2$ with stirring under aerobic conditions and then separating these products by HPLC (*19*).

Two DNA 10-mers, d(GGAA**GC**TTCC)$_2$ (**I**) and d(GGAA**AT**TTCC)$_2$ (**II**), were synthesized as representative sequences containing specific (5′-G-pyrimidine-3′) and nonspecific sites, respectively (*25*). Chemicals used in the experiments were of reagent grade or of the highest purity available.

Fluorescence Measurement of Drug−DNA Association Constants. Fluorescence spectra of the metal-free and various metallobleomycin complexes were recorded with a SLM AMINO 3400c spectrofluorometer at 25 °C. Excitation at 300 nm produced an intense emission from the bithiazole moiety at 350 nm, which was quenched upon binding with the DNA 10-mers. On the basis of the fluorescence quenching data, the association constant was determined using the following equation routinely applied to DNA binding equilibria involving (M)Blm species (*25*, *26*):

$$1/[\mathrm{(M)Blm{-}DNA}] = 1/(nK[\mathrm{DNA_o}][\mathrm{(M)Blm}]) + 1/(n[\mathrm{DNA_o}]) \quad (6)$$

The total concentration of 10-mer base pairs is [DNA$_o$] and

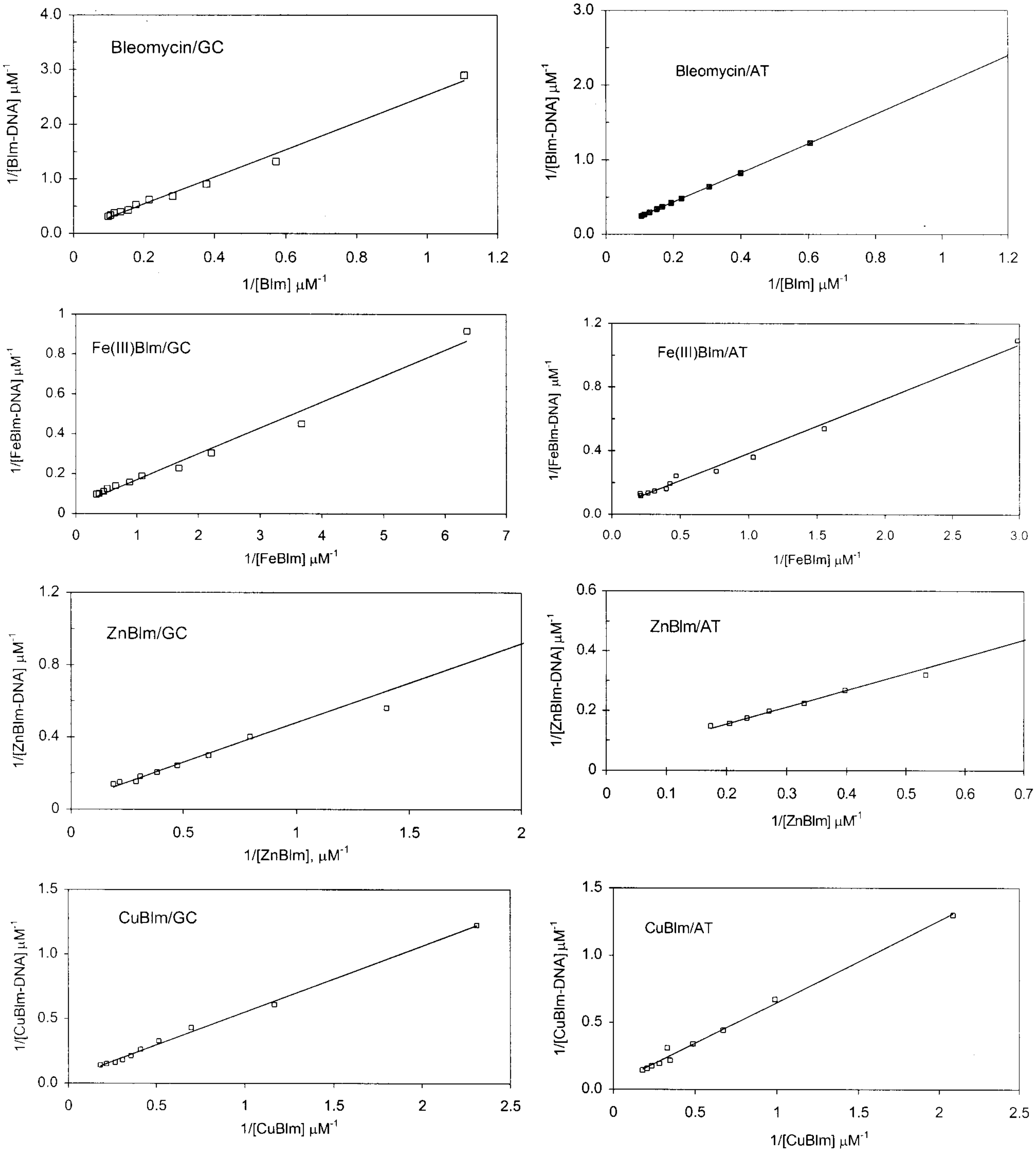

FIGURE 2: Secondary plots of fluorescence emission titrations of DNA oligomer **I** (GC) and **II** (AT) with various (M)Blms analyzed according to eq 6. Conditions: 25 μM $\mathbf{I}_o$ or $\mathbf{II}_o$ as DNA_o, 20 mM HEPES, pH 7.4 and 25 °C.

that of (M)Blm, [(M)Blm_o]; [(M)Blm] = [(M)Blm_o]$(F - F_c)/(F_b - F_c)$; and [(M)Blm−DNA] = [(M)Blm_o]$(F_b - F)/(F_b - F_c)$. In these equations, F is the fluorescent intensity of the sample after an addition of a given concentration of drug; F_b is the intensity of free (M)Blm if all of it is unbound; and F_c is the intensity when all of that concentration of (M)Blm is bound to DNA. From the analysis one can determine K, the association constant, and n, the number of binding sites per base pair.

NMR Spectroscopy. The one-dimensional ^{1}H NMR spectrum (100 MHz) of the imino proton region of **I** contains four resonances representing eight protons in the degenerate structure. Oligomer **I** was titrated with various species of Blm A_2 in 90% H_2O:10% D_2O at pH 7.4, and its imino proton spectrum examined for loss of degeneracy, indicative of slow exchange, site-specific binding of drug to DNA (*25*). On the basis of the equilibrium constants of Table 1 and the conditions of the experiment described in Figure 3, Blm was 81% bound to **I** in the one-to-one mixture of drug and DNA; the other drugs were stoichiometrically bound to **I**.

CD Spectroscopy. CD spectra were recorded at 25 °C with a Jasco 710 spectropolarimeter using a 1 mm path length, cylindrical quartz. The DNA concentration of 0.1 mM was dilute enough to permit the collection of reproducible spectra.

Table 1: Equilibrium Constants for the Association of Bleomycin Species with DNA 10-mers[a]

DNA 10-mer	I[b]		II[b]	
	K ($\times 10^5$)[c]	n[c]	K ($\times 10^5$)	n
Blm A_2	0.16 ± 0.01	0.099 ± 0.002	0.17 ± 0.03	0.101 ± 0.002
ZnBlm A_2	0.76 ± 0.16	0.099 ± 0.001	0.68 ± 0.06	0.098 ± 0.003
CuBlm A_2	0.84 ± 0.14	0.099 ± 0.001	0.63 ± 0.03	0.101 ± 0.001
Fe(III)Blm A_2	3.0 ± 0.3	0.098 ± 0.003	1.4 ± 0.4	0.100 ± 0.002
HO_2−Co(III)Blm A_2	39 ± 3	0.099 ± 0.003[d]	19 ± 4	0.099 ± 0.002[d]

[a] 20 mM HEPES buffer, pH 7.4, 25 °C. [b] **I**, d(GGAA**GC**TTCC)$_2$; **II**, d(GGAA**AT**TTCC)$_2$. [c] K = [(M)Blm−DNA]/(n[DNA][(M)Blm]); n = number of binding sites per base pair. [d] Reference *17*.

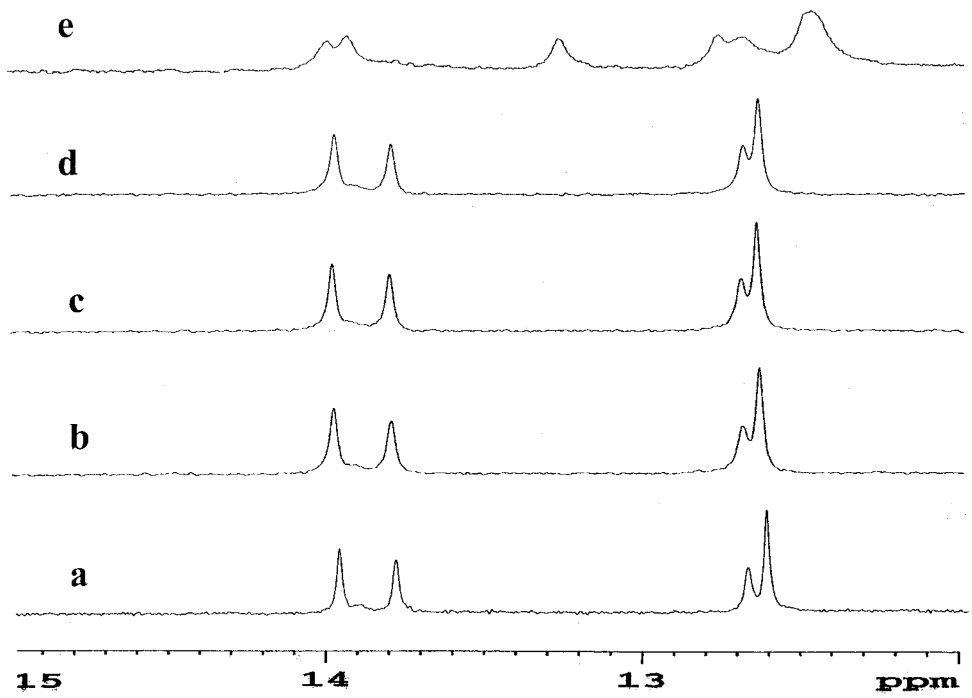

FIGURE 3: [1]H NMR spectra of **I** and drug−**I** adducts. Conditions: 0.3 mM **I** and 0.3 mM (M)Blm. Spectra: (a) **I**; (b) Blm A_2−**I** ; (c) Zn(II)Blm A_2−**I**; (d) Cu(II)Blm A_2−**I**; (e) Fe(III)Blm A_2−**I**. Conditions: solvent 90% H_2O:10% D_2O at pH 7.4.

Text figures consist of the average of four spectra recorded with 1 nm spectral resolution. Difference CD spectra were obtained by digital subtraction of the drug and DNA component spectra from the spectrum of the drug−DNA adduct. Under the conditions of the experiment, Blm was 62% bound to **I** and **II**; the others were at least 86% bound to **I** and **II**.

RESULTS

*Association Constants of MBlm A_2 Complexes with **I** and **II**.* The emission fluorescence spectra of metal-free Blm A_2 and the MBlm A_2 complexes displayed similar intense emission bands centered at 350 nm, when the molecule was excited at 300 nm in 20 mM HEPES buffer at pH 7.4. This peak has previously been attributed to fluorescence of the bithiazole chromophore (*26*). Addition of either **I** or **II** to the various Blm species quenched the fluorescence of the bithiazole moiety without shifting the emission wavelength maximum. On the basis of eq 6, the association constants and the number of binding sites per base pair for Blm and several of its metal complexes with **I** and **II** were measured in 20 mM HEPES buffer at pH 7.4 and 25 °C (Figure 2, Table 1). In all cases n was essentially 0.1, indicating that one drug molecule became associated with the DNA 10-mer. Furthermore, the constants determined for binding each form of the drug to **I** and **II** were similar, except, in almost every case, the average association constant was slightly larger for the adducts with **I**.

The association constants for the series of bleomycin species binding to either 10-mer spanned 2 orders of magnitude with Blm having the smallest constant and HO_2−Co(III)Blm A_2, the largest. It was striking that Zn- and CuBlm A_2 displayed only 4−5-fold enhancements in binding affinity in comparison with Blm A_2 and that the constant for Fe(III)Blm A_2 fell an order of magnitude below that of HO_2−Co(III)Blm A_2.

*One-Dimensional [1]H NMR Spectra of **I** with Blm A_2, ZnBlm A_2, Cu(II)Blm A_2, and Fe(III)Blm A_2.* A set of experiments was conducted to determine whether Blm A_2 or Zn-, Cu(II)-, or Fe(III)Blm A_2 binds to **I** in slow exchange on the NMR time scale as seen with the HO_2−Co(III)Blm A_2−**I** adduct (*25*). According to summary titration data shown in Figure 3, only Fe(III)Blm A_2 bound in slow exchange such that the degeneracy of the imino protons was lifted and a number of new resonances were observed (*27*). The broadening of the these peaks reflected the presence of the low-spin paramagnetic Fe(III)Blm A_2 bound to **I** (*17*).

CD Spectra of Bleomycin and Metallobleomycins. Circular dichroism spectra of (M)Blms, **I** and **II**, and their one-to-one adducts have been recorded. Difference CD spectra were

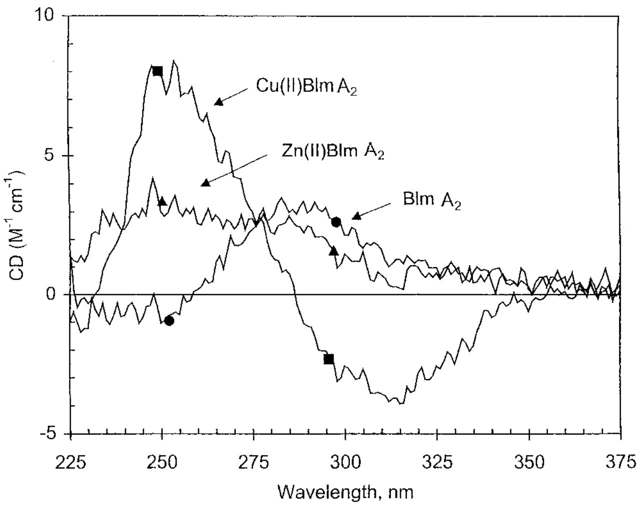

FIGURE 4: CD spectra of 0.1 mM Blm A_2 (●), ZnBlm A_2 (▲), and Cu(II)Blm A_2 (■) in 20 mM HEPES buffer at pH 7.4 and 25 °C.

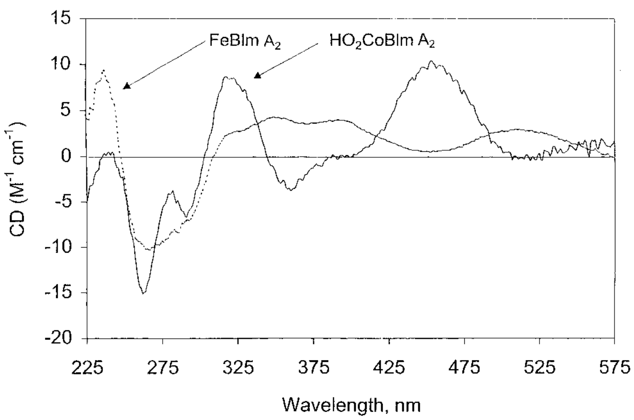

FIGURE 5: CD spectra of 0.1 mM HO_2−Co(III)Blm A_2 (solid line) and Fe(III)Blm A_2 (dotted line) in 20 mM HEPES buffer at pH 7.4 and 25 °C.

then calculated as a means to examine changes in DNA conformation resulting from DNA−(M)Blm A_2 interactions. The CD spectrum of metal-free Blm A_2 displayed a positive band at 286 nm in 20 mM HEPES buffer at pH 7.4 (Figure 4), which agrees with an earlier reported CD spectrum (*28*). This band is thought to arise from the $\pi-\pi^*$ electronic transition of the bithiazole moiety centered at 290 nm and the n−π^* transition of the 4-aminopyrimidine moiety at 285 nm (*28*, *29*).

ZnBlm A_2 displayed two positive bands at 286 and 250 nm (Figure 4). Evidently, the band at 286 nm for Blm A_2 was split upon complexation of the drug by Zn^{2+}. As such, the band at 250 nm results from the n−π^* transition of the 4-aminopyrimidine unit which has shifted upon coordination to the metal ion.

A somewhat stronger CD spectrum of CuBlm A_2 was recorded. A positive band at 250 nm and a negative band at 315 nm were observed (Figure 4). Clearly, the n−π^* transition at 250 nm in combination with the charge-transfer band at 325 nm masked the contribution from the $\pi-\pi^*$ transition of the bithiazole to the CD spectrum.

Figure 5 presents a more complicated CD spectrum of Fe(III)Blm A_2 in HEPES buffer with a positive band at 235 nm and a negative band at 265 nm. Three more positive bands are located at 350, 392, and 510 nm. The first two are considered to arise from pyrimidine to the Fe(III) charge transfer, while the third arises from Fe(III) to the pyrimidine charge transfer. In HEPES buffer, Fe(III)Blm is comprised of a mixture of low- and high-spin forms. Therefore, when phosphate is added, the structure becomes high spin, and the CD spectrum simplifies to a single band at 387 nm and a band at 510 nm (*17*). This suggested that the 350 nm band of Fe(III)Blm A_2 is sensitive to the spin state of Fe(III). A weak negative band was noted at 620 nm, which arises from the Fe(III) d−d transition.

The CD spectrum of HO_2−Co(III)Blm A_2 includes two negative troughs at 262 and 290 nm as well as positive bands at 320 and 454 nm and a negative band at 354 nm (Figure 5). On the basis of previous assignments, the 454 nm band was attributed to the charge-transfer transition of Co(III) to the pyrimidine ligand (*30*, *31*). The 320 and 354 nm bands have been assigned to the charge-transfer transitions of the pyrimidine ligand to Co(III). A weak Co(III) d−d band was also present in the spectrum.

*CD Spectra of Blm Species Bound to **I**.* The CD spectrum of **I** exhibited a strong positive band at 282 nm and a major negative band at 252 nm (Table 2 and Figure 6). This is typical of a spectrum of B-DNA (*32*). The addition of Blm A_2, ZnBlm A_2, or CuBlm A_2 only marginally perturbed this spectrum. This was readily observed in the difference spectrum, CD (mixture) − CD (**I**) − CD (drug), of each of these drug−DNA complexes (Figure 6). Blm A_2 caused virtually no change in the DNA spectrum, whereas, Zn- and CuBlm A_2 induced difference molar CD bands of less than 5 M^{-1} cm^{-1}.

Turning to Fe(III)Blm A_2 bound to **I**, the positive and negative bands of the UV CD spectrum of **I** were decreased in intensity (Figure 7a), leading to substantial difference CD bands at 250 nm (+), 269 nm (−), and 305 nm (+) (Figure 8). The first two had a difference excursion of 35 M^{-1} cm^{-1} from peak to trough. DNA adduct formation had little impact on the charge-transfer bands of Fe(III)Blm A_2, although a small enhancement of intensity between 325 and 475 nm may have occurred.

With the addition of HO_2−Co(III)Blm A_2 to **I**, the intensity of the DNA bands decreased, and their positions were blue shifted to 276 and 249 nm, respectively (Figure 7b). The charge-transfer bands of the drug were red shifted to 337 and 462 nm. Figure 8 shows the difference CD spectrum. The large positive and negative difference bands in the UV at 257 and 297 nm, primarily, represent perturbation of the DNA double helix. The difference excursion between these two bands is about 60 M^{-1} cm^{-1}. In addition, three weaker difference bands at 340, 425, and 475 nm could be assigned to changes in the charge-transfer CD bands involving the pyrimidinyl ligand and Co(III).

*CD Spectra of the Interaction of Bleomycin Species with **II**.* Structure **II** was characterized by a CD spectrum similar to that of **I** with strong bands at 281 nm (+) 250 nm (−). As with **I**, minor changes were found when Blm A_2, ZnBlm A_2, or Cu(II)Blm A_2 was added to this oligomer (Figure 9). The difference spectrum for Blm A_2−**II** resembles that of bleomycin bound to calf thymus DNA (*28*).

The UV CD spectrum of **II** was only perturbed to a small extent by Fe(III)Blm A_2 (Figure 10a). As a consequence, the difference spectrum of Fe(III)Blm A_2−**II** in Figure 11 is much weaker and also distinctly different from that for

Table 2: Circular Dichroic Features of Blm A_2, MBlm A_2, and (M)Blm A_2−DNA Adducts

structure	λ_{max} (nm)	molar ellipticity (M^{-1} cm^{-1})	structure	λ_{max} (nm)	molar ellipticity (M^{-1} cm^{-1})
Blm A_2	286	3.1	d(GGAA**GC**TTCC)$_2$ (**I**)	252	−41.5
ZnBlm A_2	250	3.0		282	74.2
	286	2.6	d(GGAA**AT**TTCC)$_2$ (**II**)	250	−62.0
CuBlm A_2	250	8.0		281	60.7
	315	−3.9	HO_2−Co(III)Blm A_2−**I**	249	−23.8
Co(III)Blm A_2	256	8.3		276	50.7
	320	3.8		302	−26.5
	354	−2.4		337	13.7
	454	8.2		462	12.3
	605	−2.5	HO_2−Co(III)Blm A_2−**II**	251	−65.9
Fe(III)Blm A_2	235	8.2		280	69.3
	265	−10.2		304	−8.7
	350	4.2		334	8.6
	392	4.0		363	−2.7
	510	3.0		461	10.9
	620	−1.2	Fe(III)Blm A_2-**I**	254	−33.8
HO_2−Co(III)Blm A_2	262	−15.1		282	55.2
	290	−6.6	Fe(III)Blm A_2-**II**	251	−66.3
	320	8.5		283	60.6
	360	−3.8			
	454	10.4			
	570	1.1			

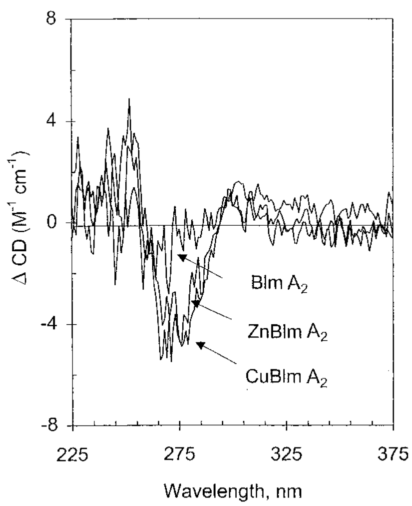

FIGURE 6: Difference CD spectra of **I** bound with Blm A_2, ZnBlm A_2, or CuBlm A_2. Difference CD = CD [(M)Blm A_2−**I**] − CD (MBlm) − CD (**I**). Conditions: 0.1 mM **I** with 0.1 mM Blm A_2, Zn(II)Blm A_2, or Cu(II)Blm A_2 in 20 mM HEPES buffer at pH 7.4 and 25 °C.

Fe(III)Blm A_2−**I**. The addition of HO_2−Co(III)Blm A_2 to **II** caused minor shifts in the UV CD spectrum with bands appearing at 280 and 250 nm (Figure 10b). As with **I**, a negative band at 300 nm was observed as well as red-shifted bands at 336 and 464 nm due to the metal center. The difference spectrum of HO_2−Co(III)Blm A_2−**II** included bands at 267 and 303 nm which spanned 40 M^{-1} cm^{-1} (Figure 11). Small difference band maxima at 331, 425, and 474 nm due to changes in the metal center as it interacted with **II** were also noted. In general, this was a weaker difference spectrum than that generated by HO_2−Co(III)-Blm A_2−**I**.

DISCUSSION

This paper describes comparative interactions of bleomycin and a number of its metal complexes with defined DNA 10-mers that differ only in the central pair of bases—one contains

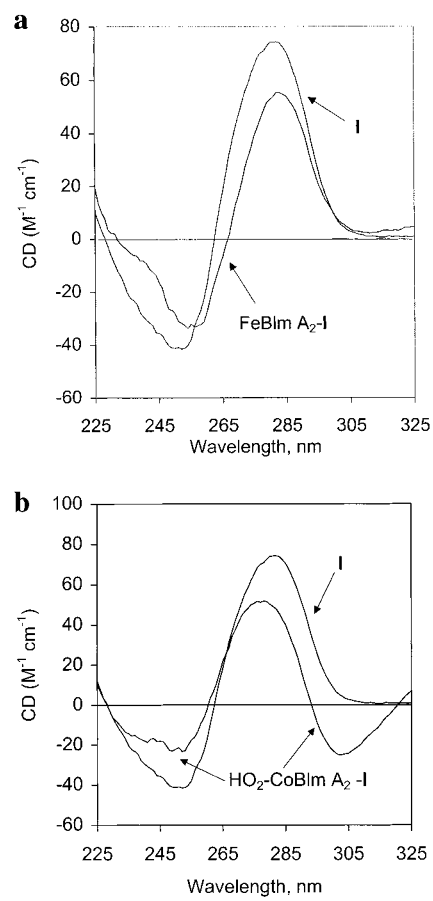

FIGURE 7: CD spectra of **I** and Fe(III)Blm A_2−**I** (a) and **I** and HO_2−Co(III)Blm A_2−**I** (b). Conditions: 0.1 mM **I** and MBlm A_2 in 20 mM HEPES buffer at pH 7.4 and 25 °C.

5′-GC-3′ (**I**), which is a specific site of reaction or binding of HO_2−Fe(III)Blm or HO_2−Co(III)Blm, respectively (*17*, *25*). In the other (**II**), 5′-AT-3′ has replaced this unit. Metal-free bleomycin displays an extended conformation which has been thought to interact with DNA primarily through its bithiazole tail. In contrast, all of the metal complexes might

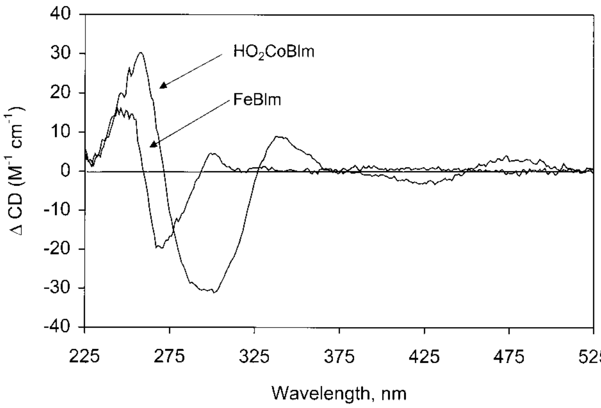

FIGURE 8: Difference CD spectra of **I** with Fe(III)Blm A_2 or HO_2-Co(III)Blm A_2. Difference CD = CD [(M)Blm A_2−**I**] − CD (MBlm) − CD (**I**). Conditions: 0.1 mM **I** and (M)Blms in 20 mM HEPES buffer at pH 7.4 and 25 °C.

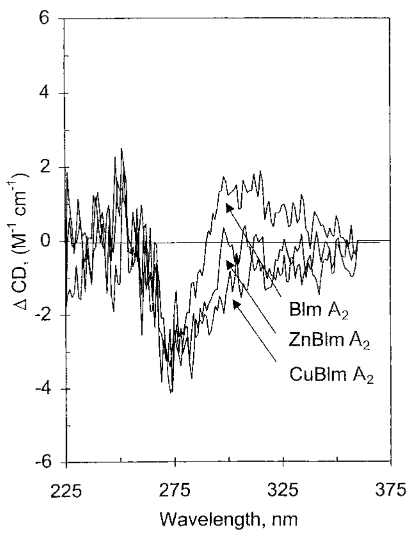

FIGURE 9: Difference CD spectra of **II** with Blm A_2, Zn(II)Blm A_2, or Cu(II)Blm A_2. Difference CD = CD [(M)Blm A_2−**I**] − CD (MBlm) − CD (**I**). Conditions: 0.1 **II** and (M)Blm in 20 mM HEPES buffer at pH 7.4 and 25 °C.

contain additional conformational determinants resulting from metal ion coordination such that they could interact with DNA through both the bithiazole tail and the metal domain−linker. HO_2-Co(III)Blm A_2, in particular, has a compact, folded structure which interacts with specific DNA 10-mers through a combination of intercalation of the bithiazole and minor groove binding of the metal domain−linker (*18*, *19*, *21*, *22*, *25*, *33*). In addition, ZnBlm is thought to bind to d(CGCTAGCG)$_2$ through minor groove interactions involving groups throughout its structure (*34*).

Previously, we have determined the association constants for the reaction of HO_2-Co(III)Blm with **I** and **II**, showing that it binds to these 10-mers with similar equilibrium constants of 3.9×10^6 and 1.9×10^6, respectively (Table 1) (*25*). Blm A_2 associates with either **I** or **II** with a substantially smaller stability constant of $1.6-1.7 \times 10^4$ according to Table 1. It is assumed that the magnitude of this interaction represents minor groove binding and/or partial intercalation of the bithiazole, electrostatic interaction between the positively charged R group with the negatively charged phosphodiester backbone of the 10-mer, and, possibly, some additional electrostatic stabilization from the net positive

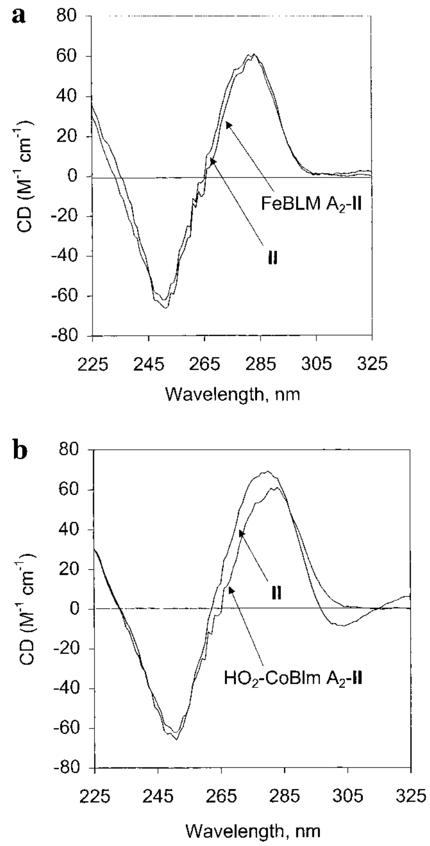

FIGURE 10: CD spectra of **II** and Fe(III)Blm A_2−**II** (a) and HO_2-Co(III)Blm A_2−**II** (b). Conditions: 0.1 mM **II** and MBlm A_2 in 20 mM HEPES buffer at pH 7.4 and 25 °C.

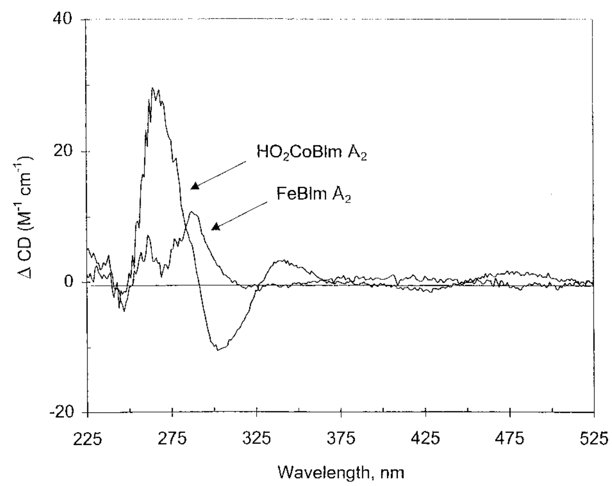

FIGURE 11: Difference CD spectra of **II** with HO_2-Co(III)Blm A_2 or Fe(III)Blm A_2. Difference CD = CD [(M)Blm A_2−**I**] − CD (MBlm) − CD (**I**). Conditions: 0.1 mM **II** and (M)Blm in 20 mM HEPES buffer at pH 7.4 and 25 °C.

charge on the metal domain region of the molecule as described below. Then, the 100−200-fold increase in association constant for the reaction of HO_2-Co(III)Blm A_2 with the two oligomers reflects the stabilization attributable to the interaction of the organized metal domain−linker with the minor groove of DNA, the chelate effect of binding both the metal domain−linker and the bithiazole tail to the oligomers, and, perhaps, some difference in the mode of binding of the bithiazole group as discussed below.

ZnBlm A_2 and CuBlm A_2 bind only 4−5 times more strongly to each oligomer than does Blm A_2. The metal-free drug contains two acidic groups with pK_a values of 4.9 and 7.5, the latter associated with an amine in the metal domain which provides about a +0.5 charge to interact with DNA at pH 7.4 (*35*). Lack of significant impact of Zn^{2+} on the stability of the Blm A_2 structure bound to **I** or **II** is likely the result of the formation of a metal domain structure that cannot interact with 5′-GC-3′ in the same manner as HO_2−Co(III)Blm A_2. Particularly, as inferred from structural studies of ^{113}CdBlm, the ligands bound to Zn^{2+} in ZnBlm A_2 only include primary amine, pyrimidine, imidazole, and, possibly, a fourth ligand at low temperature (*36*). Other NMR studies of the ZnBlm metal domain also suggest that the Zn center establishes a different coordination environment than that observed with HO_2−Co(III)Blm (*37*, *38*). Furthermore, the one published structure of ZnBlm−DNA shows that the drug adopts an extended structure in the minor groove and may not intercalate into the DNA structure with its bithiazole tail (*34*). The Zn and Co structures differ only in the metal ion bound to Blm. On the basis of previous structural studies, the apparent charge on the metal domain of ZnBlm is +1−2 which is at least as favorable for electrostatic interaction with the negatively charged DNA backbone as the +1 charge of HO_2−Co(III)Blm (*36*−*38*). Thus, it is concluded that the two metal domain conformations are distinct and this difference is likely to account for the lack of significant enhancement of binding of ZnBlm A_2 to **I** or **II** relative to Blm A_2.

This explanation cannot apply to CuBlm A_2. It has already been established that Cu−P3A, a fragment of CuBlm A_2 which essentially represents the deglyco metal domain, has the same constellation of in-plane and axial ligands as does HO_2−Co(III)Blm A_2. Consequently, their metal domains have the same net charge. According to the X-ray structure of Cu−P3A, the ligand wraps around Cu(II) with the chirality opposite to that established by the metal domain of HO_2−Co(III)Blm A_2 (*18*). As such, CuBlm A_2 cannot form the specific hydrogen bond interactions between a ring nitrogen and amine substituent of its pyrimidinyl ligand and 2-amino and N3 sites of guanine observed in the HO_2−Co(III)Blm A_2−**I** adduct (*20*, *21*, *25*). It is unclear why there should be a difference in chirality between Cu- and Co(III)Blms and whether, in fact, the chirality of Cu−P3A is the same as in CuBlm A_2. Nevertheless, it is hypothesized that this difference causes the divergent binding constants for the binding of CuBlm A_2 and HO_2−Co(III)Blm A_2 with **I** and **II** and the lack of impact of CuBlm A_2 on the CD spectrum of **I**.

Fe(III)Blm A_2 shows enhanced binding stability with **I** and **II** in comparison with Zn- and CuBlm A_2, but the contribution of the metal domain to its association constants remains only one-tenth that of the cobalt complex. This difference was unexpected because qualitative similarities have been noted between the DNA-based chemistry of Fe- and CoBlms. For example, both of the above structures interact specifically with **I** in the slow exchange regime on the NMR time scale, whereas they bind in fast exchange to **II** (Figure 3) (*17*, *27*). In addition, phosphate bound to Fe(III)Blm is only displaced upon binding to **I**, which converts the high-spin structure into a low-spin adduct (*27*). Likewise, acetate bound to Co(III)Blm is displaced upon binding to **I**, but not **II,** because the rigorous steric requirements of forming the Co(III)Blm−**I** complex cannot be met with acetate coordinated to Co(III) (unpublished information). Furthermore, both O_2−Fe(II)Blm and O_2−Co(II)Blm are stabilized to some extent by **I** in comparison with **II** (*17*). The metal domain of Fe(III)Blm presumably has the same or a larger positive charge as HO_2−Co(III)Blm, depending on whether hydroxide or water is bound to Fe(III) in its sixth, axial coordination site. Recent ESR studies of the orientation of Fe(III)Blm on DNA fibers concluded that the metal domain binds with approximately the same angle between the metal coordination plane and the helix axis as seen in the HO_2−Co(III)Blm A_2−DNA oligomer structures (*33*, *40*). Considering the parallel behavior of these MBlms with DNA, the reason for their difference in binding constants is not evident.

A striking result is that **I** and **II** bind Blm A_2 or each of the various metallobleomycins with similar, if not identical, association constants (Table 1). This might be expected for the metal-free drug and its Zn and Cu complexes because they do not appear to be able to form site-selective adducts with DNA that discriminate between **I** and **II**. In contrast, Fe(III)Blm A_2 and HO_2−Co(III)Blm A_2 make specific complexes with **I** but not with **II,** based on NMR titration data (Figure 3 and refs *17* and *25*). Thus, one might have anticipated larger differences in their association constants with the two oligomers.

The guanine of GC or GT recognition sites establishes two hydrogen bonds with the pyrimidinyl moiety of HO_2−Co(II)Blm A_2 (*21*, *22*). One of the two hydrogen bonds cannot be formed with **II**, in which A has replaced G. In work to be published elsewhere, we find two other hydrogen bonds between the drug and **I**, each involving the bases opposite the 5′-GC-3′ site. The first links the drug pyrimidinyl acetamido NH_2 group and the carbonyl of C base paired to G at the site (Figure 1) (*33*). The other involves N7 of G paired with C in the major groove and NH of the amide connecting the R group to bleomycinic acid. These should also form at the AT site. If so, then three of the four hydrogen bonds that are observed in the HO_2−Co(III)Blm A_2−**I** complex can also form when the AT sequence replaces GC, consistent with only a small reduction in thermodynamic affinity of HO_2−Co(III)Blm for **II** in comparison to **I**.

The difference in the association constants for the binding of various MBlm A_2 species with **I** is not necessarily correlated with the kinetic exchange rate, as seen by the 10-fold difference in the affinity of Fe(III)Blm A_2 and HO_2−Co(III)Blm A_2 for **I** (Table 1) in contrast to their qualitative similarity in chemical exchange properties as measured by NMR spectroscopy (Figure 3). Furthermore, neither NO−Fe(II)Blm nor O_2−Co(II)Blm binds to **I** in slow exchange (unpublished information). Nevertheless, these structures as well as Fe(III)Blm appear to establish fixed-metal domain conformations with respect to DNA that are closely related to that for HO_2−Co(III)Blm in the NMR structure (*33*, *40*, *41*). In addition, recent experiments have shown that HO_2−Co(III) deglycobleomycin A_2 can associate in slow exchange with a DNA 10-mer containing a 5′-GC-3′ site, forming the same adduct structure as HO_2−Co(III)Blm A_2 despite exhibiting an association constant with the oligomer that is only about 3% of that for the native structure (2×10^5) (*42*). Thus, results to date indicate that the underlying chemistry of these metallobleomycins which distinguishes GC and AT sites is subtle and may be partially a kinetic phenomenon in which the lifetime of the drug−G−pyrimidine adduct is longer than that at other sites.

The properties of binding of metallobleomycins to **I** and **II** have also been examined by CD spectroscopy. Drugs and DNA 10-mers, themselves, display optical activity (Table 2). This study focused on changes induced in the circular dichroism spectrum of either oligomer or drug upon adduct formation. These were readily detected in difference spectra. The difference CD spectrum of Blm A_2 with **I** was almost flat (Figure 6). Thus, intercalation or another mode of interaction of the bithiazole tail of the drug with DNA such as minor groove binding did not significantly perturb the structure of these 10-mers. The same conclusion was reached upon review of the difference CD spectra of ZnBlm A_2 or CuBlm A_2 bound to **I** (Figure 6). An interpretation based on comparative stability constants, NMR exchange rate, and CD spectroscopy is that Blm A_2, ZnBlm A_2, and CuBlm A_2 largely bind with DNA through similar interactions including the bithiazole tail moiety and positive charge associated with the metal domain in Blm A_2 and Zn- and CuBlm A_2. Considering the structure of ZnBlm bound in fast exchange to $d(CGCTAGCG)_2$, which shows the drug extended from the metal domain to the R group tail in the DNA minor groove, it is hypothesized that each of these forms of Blm is a minor groove binder that may also gain some stability through partial intercalation between base pairs. Results of a full Raman spectroscopic analysis of Blm bound to calf thymus DNA are also consistent with minor groove binding of Blm as well as some contribution from intercalation (*43*, *44*).

Fe(III)Blm A_2 diminished the UV circular dichroism spectrum of **I** (Figure 7a) such that the adduct with **I** displayed a significant difference CD spectrum, indicative of perturbation of the DNA structure through drug binding (Figure 8). Since Fe(III)Blm A_2 is distinguished from Zn- and CuBlm A_2 by the nature of the bound metal ion, it is evident that Fe(III) complexation alters the structure of the drug so that it exerts an easily measurable effect on DNA (*17*, *24*).

The peculiar behavior of HO_2−Co(III)Blm A_2 when compared to Fe(III)Blm A_2 was indicated by its larger adduct association constants with both oligomers and by its impact on the Cd spectra of **I** and **II**. This form of the drug caused the largest perturbation in the spectra of both 10-mers (Figures 7a, 8, 10a, and 11). These differences along with the finding that O_2−Co(II)Blm displays more stability when bound to DNA than O_2−Fe(II)Blm indicate that subtle differences in drug−DNA binding may exist among the structures (*16*, *17*).

Decrease in the intensity of the UV CD bands of double-helical DNA is a clear indicator of reduction in stacking interactions between adjacent bases (*32*). Such perturbations are seen in the spectra of HO_2−Co(III)Blm A_2 and Fe(III)-Blm A_2 bound to **I** (Figure 7). Hypothetically, the intercalation of the bithiazole into the DNA structure, which necessarily separates the base pairs (*21*−*23*, *27*), is responsible for the loss of CD intensity in the UV region (*27*, *40*).

The bithiazole unit is common to Blm A_2 and all of the metallobleomycins; nevertheless, its intercalative binding is correlated only with specific metal domain interaction with DNA by HO_2−Co(III)Blm A_2 and Fe(III)Blm A_2. To account for this observation, it is hypothesized that DNA adduct formation by HO_2−Co(III)Blm A_2 and Fe(III)Blm A_2 cooperatively involves the metal domain and bithiazole regions of the metallobleomycin structure. In the absence of the capacity of the metal domain to associate through specific hydrogen bonds with guanine at the recognition site, minor groove binding becomes more significant as seen with Blm and ZnBlm in other studies (*34*, *43*, *44*).

Finally, the circular dichroic properties of the cobalt center were altered by both 10-mers. The subtle effects observed in the difference spectra emphasize the interaction of the metal domain with DNA and its association with both G and A of the central dinucleotides **I** and **II** (Figures 7 and 9). The difference CD bands above 300 nm are hypothesized to reflect the impact of hydrogen bonding of the Co-bound pyrimidinyl group to the guanine or adenine ring nitrogen (N3) on the charge-transfer bands of the metal complex.

ACKNOWLEDGMENT

We thank Dr. Vaughn Jackson for the use of his spectropolarimeter and Dr. Sally Twining for making her spectrofluorometer available to us.

REFERENCES

1. Umezawa, H., Ishizuka, M., Kimura, K., Iwanaga, J., and Takeuchi, T. (1968) *J. Antibiot. A21*, 592−602.
2. Radtke, K., Lornitzo, F. A., Byrnes, R. W., Antholine, W. E., and Petering, D. H. (1994) *Biochem. J. 302*, 655−664.
3. Sausville, E. A., Peisach, J., and Horwitz, S. B. (1976) *Biochem. Biophys. Res. Commun. 73*, 814−822.
4. Povirk, L. F., Wubter, W., Köhnlein, W., and Hutchinson, F. (1977) *Nucleic Acids Res. 4*, 3573−3580.
5. Suzuki, T., Nagai, K., Yamaki, H., Tanaka, N., and Umezawa, H. (1969) *J. Antibiot. 22*, 446−448.
6. Petering, D. H., Byrnes, R. W., and Antholine, W. E. (1990) *Chem.*−*Biol. Interact. 73*, 133−182.
7. Burger, R. M., Peisach, J., and Horwitz, S. B. (1981) *J. Biol. Chem. 256*, 11636−11644.
8. Kuramuchi, A., Takahashi, K., Takita, T., and Umezawa, U. (1981) *J. Antibiot. 34*, 576−582.
9. Claussen, C. A., and Long, E. C. (1999) *Chem. Rev. 99*, 2797−2816.
10. D'Andrea, A. D., and Haseltine, W. A. (1978) *Proc. Natl. Acad. Sci. U.S.A. 75*, 3608−3612.
11. Sugiura, Y., and Suzuki, T. (1982) *J. Biol. Chem. 257*, 10544−10546.
12. Byrnes, R. W., Templin, J., Sem, D., Lyman, S., and Petering, D. H. (1990) *Cancer Res. 50*, 5275−5286.
13. Lehmann, T. E., Ming, L.-J., Rosen, M. E., and Que, L., Jr. (1997) *Biochemistry 36*, 2807−2816.
14. Xu, R. X., Antholine, W. E., and Petering, D. H. (1992) *J. Biol. Chem. 267*, 944−949.
15. Xu, R. X., Antholine, W. E., and Petering, D. H. (1992) *J. Biol. Chem. 267*, 950−955.
16. Fulmer, P., and Petering, D. H. (1994) *Biochemistry 33*, 5319−5327.
17. Fulmer, P., Zhao, C., Li, W., DeRose, E., Antholine, W. E., and Petering, D. H. (1997) *Biochemistry 36*, 4367−4374.
18. Xu, R X., Nettesheim, D., Otvos, J. D., and Petering, D. H. (1994) *Biochemistry 33*, 907−916.
19. Wu, W., Vanderwall, D. E., Lui, S. M., Tang, X.-J., Turner, C. J., Kozarich, J. W., and Stubbe, J. (1996) *J. Am. Chem. Soc. 118*, 1268−1280.
20. Petering, D. H., Mao, Q., Li, W., DeRose, E., and Antholine, W. E. (1996) *Met. Ions Biol. Syst. 33*, 619−648.
21. Wu, W., Vanderwall, D. E., Turner, C. J., Kozarich, J. W., and Stubbe, J. (1996) *J. Am. Chem. Soc. 118*, 1281−1294.
22. Vanderwall, D. E., Lui, S. M., Wu, W., Turner, C. J., Kozarich, J. W., and Stubbe, J. (1997) *Chem. Biol. 4*, 373−387.

23. Caceres-Cortes, J., Sugiyama, H., Ikudome, K., Saito, I., and Wang, A. H.-J. (1997) *Eur. J. Biochem. 244*, 818−828.
24. Sam, J. W., Takahashi, S., Lippai, I., Peisach, J., and Rousseau, D. L. (1998) *J. Biol. Chem., 273*, 16090−16097.
25. Mao, Q., Fulmer, P., Li, W., DeRose, E. F., and Petering, D. H. (1996) *J. Biol. Chem. 271*, 6185−6191.
26. Chien, M., Grollman, A. P., and Horwitz, S. B. (1977) *Biochemistry 16*, 3641−3647.
27. Li, W., Xia, C., Antholine, W. E., and Petering, D. H. (submitted for publication).
28. Krueger, W. C., Pschigoda, L. M., and Reusser, F. (1973) *J. Antibiot. 8*, 424−428.
29. Dabrowiak, J. C. (1982) in *Advances in Inorganic Biochemistry* (Eichhorn, G. L., and Marzilli, L. G., Eds.) Vol. 4, pp 69−113, Elsevier, Amsterdam.
30. Garnier-Suillerot, A., Albertini, J. P., and Tosi, L. (1981) *Biochem. Biophys. Res. Commun. 102*, 499−506.
31. Pickens., S. R., Martell, A. E., McLendon, G., Lever, A. B. P., and Gray, H. B. (1978) *Inorg. Chem. 17*, 2190−2192.
32. Johnson, W. C., Jr. (1996) in *Circular Dichroism and the Conformational Analysis of Biomolecules* (Fasman, G. D., Ed.) pp 433−468, Plenum Press, New York.
33. Zhao, C., Mao, Q., Xia, C., Försterling, H., DeRose, E., and Petering, D. H. (submitted for publication).
34. Manderville, R. A., Ellena, J. F., and Hecht, S. M. (1995) *J. Am. Chem. Soc. 117*, 7891−7903.
35. Chen, D. M., Hawkins, B. I., and Glickson, J. D. (1977) *Biochemistry 16*, 2731−2738.
36. Otvos, J. D., Antholine, W. E., Wehrli, S., and Petering, D. H. (1996) *Biochemistry 35*, 1458−1465.
37. Calafat, A. M., Won, H., and Marzilli, L. G. (1997) *J. Am. Chem. Soc. 119*, 3656−3664.
38. Akkerman, M. A., Haasnoot, C. A. G., and Hilbers, C. W. (1988) *Eur. J. Biochem. 173*, 211−225.
39. Iitaka, Y., Nakamura, H., Nakatani, T., Muraoka, Y., Fujii, A., Takita, T., and Umezawa, H. (1978) *J. Antibiot. 31*, 1070−1072.
40. Chikira, M., Iiyama, T., Sakamoto, K., Antholine, W. E., and Petering, D. H. (2000) *Inorg. Chem. 39*, 1779−1786.
41. Chikira, M., Antholine, W. E., and Petering, D. H. (1989) *J. Biol. Chem. 264*, 21478−21480.
42. Wu., W., Vanderwall, D. E., Teramoto, S., Man Lui, S., Hoehn, S. T., Tang, X.-J., Turner, C. J., Boger, D., Kozarich, J. W., and Stubbe, J. (1998) *J. Am. Chem. Soc. 120*, 2239−2250.
43. Rajani, C., Kincaid, J., and Petering, D. H. (2000) *Biopolymers* (in press).
44. Rajani, C., Kincaid, J., and Petering, D. H. (2000) *Biopolymers* (in press).

BI001915T